BIOCHEMISTRY
including biophysical chemistry & molecular biology

Article

pubs.acs.org/biochemistry

Ring Flips Revisited: ^{13}C Relaxation Dispersion Measurements of Aromatic Side Chain Dynamics and Activation Barriers in Basic Pancreatic Trypsin Inhibitor

Ulrich Weininger, Kristofer Modig, and Mikael Akke*

Department of Biophysical Chemistry, Center for Molecular Protein Science, Lund University, P.O. Box 124, SE-221 00 Lund, Sweden

Supporting Information

ABSTRACT: Intramolecular motions of proteins are critical for biological function. Transient structural fluctuations underlie a wide range of processes, including enzyme catalysis, ligand binding to buried sites, and generic protein motions, such as 180° rotation of aromatic side chains in the protein interior, but remain poorly understood. Understanding the dynamics and molecular nature of concerted motions requires characterization of their rates and energy barriers. Here we use recently developed ^{13}C transverse relaxation dispersion methods to improve our current understanding of aromatic ring flips in basic pancreatic trypsin inhibitor (BPTI). We validate these methods by benchmarking ring-flip rates against the three previously characterized cases in BPTI, namely, Y23, Y35, and F45. Further, we measure conformational exchange for one additional aromatic ring, F22, which can be interpreted in terms of a flip rate of 666 s^{-1} at 5 °C. Upon inclusion of our previously reported result that Y21 also flips slowly [Weininger, U., et al. (2013) *J. Phys. Chem. B 117*, 9241−9247], the ^{13}C relaxation dispersion experiments thus reveal relatively slow ring-flip rates for five of eight aromatic residues in BPTI. These results are in contrast with previous reports, which have estimated that all rings, except Y23, Y35, and F45, flip with a high rate at ambient temperature. The ^{13}C relaxation dispersion data result in an updated rank order of ring-flip rates in BPTI, which agrees considerably better with that estimated from a recent 1 ms molecular dynamics trajectory than do previously published NMR data. However, significant quantitative differences remain between experiment and simulation, in that the latter yields flip rates that are in many cases too fast by 1−2 orders of magnitude. By measuring flip rates across a temperature range of 5−65 °C, we determined the activation barriers of ring flips for Y23, Y35, and F45. Y23 and F45 have identical activation parameters, suggesting that the fluctuations of the protein core around these residues are similar in character. Y35 differs from the other two in its apparent activation entropy. These results might be rationalized by the fact that Y23 and F45 are located in the same region of the structure while Y35 is remote from the other two rings. As indicated by our new results for the exceptionally well-characterized protein BPTI, ^{13}C relaxation dispersion experiments open the possibility of studying ring flips in a range of cases wider than that previously possible.

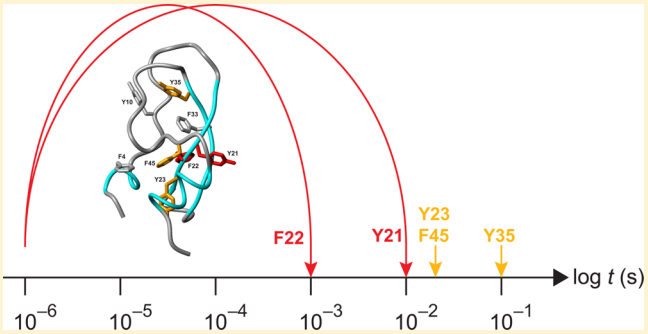

Proteins continuously undergo dynamic processes distributed over a wide range of time scales. Buried functional sites can be accessed as a consequence of transient structural fluctuations. Aromatic ring flips are a hallmark example of such "breathing motions" and have a very long history in biophysics, dating back some 35 years to milestone studies that shifted the view of proteins as static structures to dynamic systems.[1,2]

Despite the long history of using aromatic ring flips as a probe of protein dynamics, only a handful of cases in which the rates of ring flips have actually been measured have been reported. Instead, the appearance of the nuclear magnetic resonance (NMR) spectrum has often been taken as a proxy for the rate of ring flips,[1] as outlined further below. The list of actual ring-flip measurements includes basic pancreatic trypsin inhibitor (BPTI),[1,3−6] cytochrome *c*,[7−9] yeast iso-2-cytochrome *c*,[10] hen lysozyme,[11] histidine-containing phosphocarrier protein (HPr),[12] and xylanase.[13] In some of these studies, the ring-flip kinetics have been measured as a function of temperature or pressure, yielding activation energies[1,6,8,10,12] or activation volumes,[3,5,12] respectively. Previous studies have typically employed ^{1}H NMR line shape analyses or longitudinal-exchange spectroscopy, and a great majority of these report on slow ring flips (k_{flip} < 10^3 s^{-1}). Very slow ring flips at low temperatures have been measured for BPTI using ^{1}H−^{1}H NOESY experiments.[6]

Usually, the symmetric pairs of nuclei in the aromatic rings of Tyr and Phe give rise to single signals in the NMR spectrum,

Received: April 16, 2014
Revised: July 1, 2014
Published: July 1, 2014

indicating that the ring-flip rate is fast compared to the chemical shift difference between the two nuclei on either side of the ring. On the basis of the statistical distribution of chemical shifts listed in the BioMagResBank[14] for the δ and ε nuclei in Tyr and Phe, it might be expected that an exchange-averaged peak is indicative of a ring-flip rate on the order of 10^3-10^5 s^{-1} at ambient temperature.[6] However, it should be kept in mind that a single resonance also can arise as a consequence of chemical shift degeneracy between the two sides of the ring, and that the observation of a single resonance does not carry any information on the absolute rate of ring rotation. As a case in point, we recently demonstrated that Y21 of BPTI undergoes slow ring flips (k_{flip} < 100 s^{-1}) even though the $^1H-^{13}C$ correlation spectrum shows only a single peak for each symmetric pair of nuclei in this aromatic ring.[15]

In the past decade, powerful NMR methods have been developed to study exchange phenomena in proteins and other biomolecules. Relaxation dispersion experiments performed as a function of the refocusing frequency allow investigations of dynamics on the microsecond to millisecond time scales, in terms of the exchange rate constants, the relative populations of the exchanging states, and the chemical shift difference between these.[16−18] This type of experiment further has the advantage that, contrary to line shape analysis, it is not influenced by static magnetic field inhomogeneity. In addition, heteronuclear NMR spectroscopy usually is less affected by spectral overlap than are experiments based solely on ^1H. Relaxation dispersion experiments targeting aromatic rings have been hampered previously by the large coupling between adjacent ^{13}C sites, but isotope labeling strategies that yield specific ^{13}C enrichment now make it possible to use aromatic ^{13}C spins as probes of ring-flip dynamics.[19−21] Recently, we developed a suite of relaxation dispersion experiments tailored specifically for aromatic ^{13}C spins.[22,23]

Rotations of aromatic rings located in the hydrophobic core of proteins require sizable activation volumes, the creation of which involves coordinated movement of surrounding residues.[24,25] Little is known about the mechanisms of aromatic ring flips, but sufficiently long molecular dynamics (MD) simulations are now starting to shed light on these relatively infrequent events. As the time scales that can be accessed by MD simulations approach those covered by NMR methods for studying conformational exchange, the opportunity to critically appraise force field performance and simulation methods by validating simulations against experiment arises.[26−28]

Here we reinvestigate aromatic ring flips in BPTI using L-optimized TROSY-selected ^{13}C relaxation dispersion experiments as a function of temperature. The dynamic behaviors of slowly flipping rings Y23, Y35, and F45 are generally well reproduced, although slight differences are observed for the flip rates of Y23 and the activation barriers of Y35. We also measured, for the first time, a relatively slow exchange rate for F22. Together with our previous result that Y21 also has a slow flip rate,[15] we thus report an expanded list of slowly flipping aromatics in BPTI that agrees well on a qualitative level with a recent 1 ms MD trajectory.[26]

MATERIALS AND METHODS

NMR Spectroscopy. Aromatic ^{13}C L-TROSY-CPMG[22] and ^{13}C L-TROSY-$R_{1\rho}$[23] relaxation dispersion experiments were performed on an 8 mM sample of nonlabeled BPTI in 90% H_2O and 10% D_2O (pH 7.1); the protein concentration was thus similar to those employed in previous studies, which ranged between 6 and 10 mM.[1,6] CPMG relaxation dispersion experiments were conducted at static magnetic field strengths (B_0) of 11.7 and 14.1 T and temperatures of 5, 15, 25, 35, 45, and 55 °C. CPMG refocusing frequencies (ν_{cp}) were 33, 67, 100, 167, 233, 333, 433, 533, 667, 833, and 1000 Hz at all temperatures, except at 55 °C where they were set to 50, 100, 200, 300, 400, 600, 700, 800, 900, and 1000 Hz. The B_1 field strengths of the CPMG refocusing pulses were 12800 Hz (11.7 T) and 11000 Hz (14.1 T). $R_{1\rho}$ relaxation dispersion experiments were conducted at 11.7 T and at 55 and 65 °C, using B_1 field strengths of 807, 973, 1225, 1583, 1944, 2397, 3109, 4014, and 5018 Hz. The B_1 field strengths of the spin-lock were calibrated by measuring the residual $^1J_{HC}$ couplings in an aromatic $^1H-^{13}C$ HSQC spectrum acquired with continuous-wave decoupling during acquisition.[17] The temperature was calibrated using a copper-constantan thermocouple in an NMR tube containing a water/ethanol mixture.

Data Analysis. Spectra were processed using NMRPipe[29] and analyzed using NMRView.[30] Relaxation dispersions were fit to the Carver−Richards equation[31,32] in the case of intermediate to fast exchange. In the slow-exchange regime, relaxation dispersions were fit to the following equation:[33,34]

$$R_{2,obs} = R_{2,0} + k_{flip}[1 - \mathrm{sinc}(\gamma B_0 \Delta\delta/\nu_{cp})] \quad (1)$$

where $R_{2,0}$ is the exchange free transverse relaxation rate, assumed to be identical for the two sites, γ is the gyromagnetic ratio, and $\Delta\delta$ is the chemical shift difference between the two sites. Data modeling utilized the Levenberg−Marquardt nonlinear least-squares optimization algorithm[35] implemented in MATLAB. All data were analyzed by using fixed populations ($p_1 = p_2 = 0.5$) and treating $\Delta\delta$ as either a free parameter ($\Delta\delta_{disp}$) or fixed at the value ($\Delta\delta_{spectra}$) measured from HSQC spectra under slow-exchange conditions. In all cases where separate resonances were observed for the two sides of a ring, $\Delta\delta$ was independent of temperature to within ±0.01 ppm. $R_{1\rho}$ relaxation data acquired at 55 and 65 °C were fit simultaneously to the general equation for symmetric exchange derived by Miloushev and Palmer,[36] while imposing the constraint k_{ex}(65 °C) > k_{ex}(55 °C). Activation barriers of the ring flips were determined by nonlinear regression of the flip rates ($k_{flip} = k_{ex}/2$) on temperature T, using either the Arrhenius or Eyring equation. The Arrhenius equation was parametrized as

$$k_{flip} = A \times \exp(-E_a/RT) \quad (2)$$

where A is the pre-exponential factor, E_a is the activation energy, and R is the gas constant. The Eyring equation was parametrized as

$$k_{flip} = (k_B T/h) \times \exp[-(\Delta H^{\ddagger} - T\Delta S^{\ddagger})/RT] \quad (3)$$

where k_B and h are Boltzmann's constant and Planck's constant, respectively, and $\Delta H^{\ddagger}$ and $\Delta S^{\ddagger}$ are the activation enthalpy and activation entropy, respectively. The Eyring equation was thus applied under the assumption that the transmission coefficient equals 1. Errors in the fitted parameters were estimated using Monte Carlo simulations;[35] the reported errors correspond to one standard deviation.

RESULTS AND DISCUSSION

^{13}C Relaxation Dispersion Experiments Allow Measurement of Previously Uncharacterized Ring Flips. We recorded L-TROSY CPMG[22] relaxation dispersion profiles for aromatic $^{13}C^{\delta}$ and $^{13}C^{\varepsilon}$ spins at natural abundance and five

dx.doi.org/10.1021/bi500462k | Biochemistry 2014, 53, 4519−4525

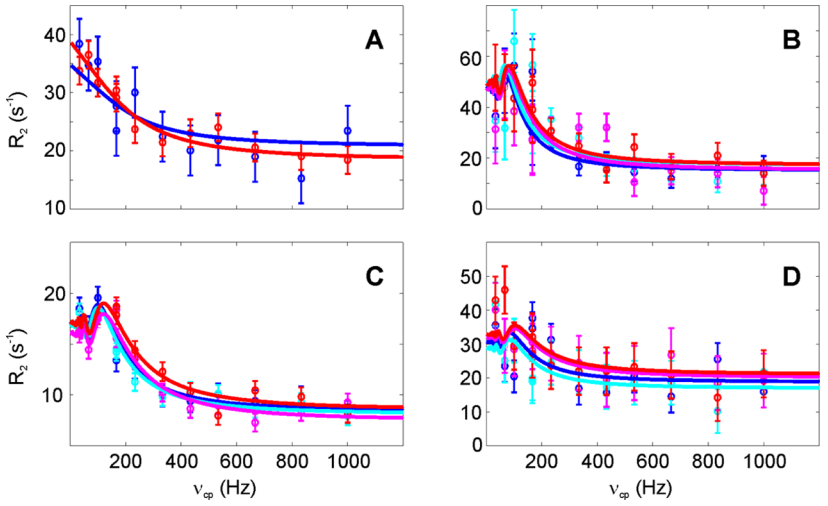

Figure 1. Representative ^{13}C CPMG relaxation dispersion profiles acquired at static magnetic field strengths of 11.7 T (blue and cyan) and 14.1 T (red and magenta): (A) F22ε at 5 °C, (B) Y23ε at 15 °C, (C) Y35ε at 35 °C, and (D) F45δ at 5 °C. Two colors (blue and cyan or red and magenta) are used in those cases where separate signals are observed in the spectra for each pair of δ or ε nuclei. All data acquired for a given residue and temperature were fit together, using fixed populations ($p_1 = p_2 = 0.5$) and free chemical shift difference(s) ($\Delta\delta_{disp}$). The resulting exchange rates (k_{ex}) are (A) (13 ± 4) × 10^2, (B) 64 ± 7, (C) 17.3 ± 0.7, and (D) 24 ± 4 s^{-1}.

different temperatures, ranging from 5 to 55 °C. BPTI contains four phenylalanine and four tyrosine residues. Five of these eight residues (Y21, F22, Y23, Y35, and F45) showed evidence of exchange in the ^{13}C relaxation dispersion experiments (Figure 1, Figures S1 and S2 of the Supporting Information, and ref 15). Three of these (Y23, Y35, and F45) have previously been observed to undergo slow ring flips.[1] The slow exchange of these three residues is manifested in the $^1H-^{13}C$ correlation spectrum at lower temperatures, which displays separate resonances for the two nuclei on the opposite sides of the aromatic ring (Figure S3 of the Supporting Information). Here, we establish that also F22 experiences a relatively slow exchange process (Figure 1A), which we tentatively interpret as a ring flip, even though only a single, exchange-averaged resonance is observed for each pair of δ or ε nuclei across the range of temperatures studied here. We have previously demonstrated that Y21 undergoes slow ring flips (k_{flip} < 100 s^{-1} at 35 °C) by analyzing its anomalous, "upside-down" CPMG relaxation dispersion profiles that arise from strong $^1H-^1H$ couplings between the proton attached to the monitored ^{13}C nucleus and its vicinal neighbor (attached to ^{12}C).[15] Of note, Y21 also exhibits degenerate ^1H and ^{13}C chemical shifts for both the δ and ε nuclei. Thus, the ^{13}C CPMG relaxation dispersion experiment has revealed two additional residues exhibiting relatively slow ring flips in BPTI, besides the three previously well-documented cases.

The exchange dynamics of all five residues showing ^{13}C relaxation dispersion can be adequately described as a two-state process with equal populations ($p_1 = p_2 = 0.5$). In the case of the four residues showing canonical relaxation dispersion profiles (F22, Y23, Y35, and F45), both the exchange rate constant and the chemical shift difference could be determined by fitting these parameters to the data using eq 1 or the Carver–Richards equation[31,32] (Figure 1). Table 1 lists the fitted rate constants. The rate constants were identical within error regardless of whether the chemical shift differences were included as free parameters ($\Delta\delta_{disp}$) of the fit (Figure S1 of the Supporting Information) or fixed at the values ($\Delta\delta_{spectra}$) measured in the $^1H-^{13}C$ correlation spectra (Figure S2 of the Supporting Information), as summarized in Table S1 of the Supporting Information. Moreover, $\Delta\delta_{disp}$ agrees well with $\Delta\delta_{spectra}$ (Figure S4 of the Supporting Information), indicating that the method yields robust results. The fitted rate constants obtained for Y23, Y35, and F45 serve to validate the ^{13}C L-TROSY-CPMG[22] relaxation dispersion method by benchmarking against previous results.[1,6] We generally obtain good agreement with earlier data, which were obtained by ^1H line shape analysis. The largest deviations are observed for Y23, where the previously reported rates are lower by a factor of approximately 4–5 (see also Figure 2).

Table 1. Exchange Rate Constants Determined by ^{13}C Relaxation Dispersion Experiments[a]

residue	T (°C)	k_{ex} (s^{-1})
F22ε	5	(1.3 ± 0.4) × 10^3
Y23ε	5	18 ± 3
	15	64 ± 7
	55	(4.7 ± 0.9) × 10^3
	65	(19 ± 2) × 10^3
Y35ε	35	17.3 ± 0.7
	45	63 ± 4
	55	118 ± 10
F45δ	5	24 ± 4
	55	(14 ± 4) × 10^3
	65	(20 ± 3) × 10^3

[a]Parameters were obtained by nonlinear least-squares fits against the relaxation dispersion data acquired using CPMG (5–45 °C) or spin-lock (55–65 °C) refocusing elements. $\Delta\delta$ was included as a fixed parameter in the fit, except for F22, which is in the fast-exchange regime.

The exchange rate measured for F22 $^{13}C\varepsilon$ corresponds to a k_{flip} of (6.7 ± 1.8) × 10^2 s^{-1} at 5 °C. While it cannot be ascertained at present that the measured exchange is due to ring flips, several observations support this interpretation. First, the F22δ cross-peak is also broadened, but the F22ζ cross-peak is not, in agreement with the expected outcome of a ring flip, which modulates the chemical shifts of the δ and ε nuclei but leaves that of the ζ nucleus unaffected. Unfortunately, F22δ is

dx.doi.org/10.1021/bi500462k | Biochemistry 2014, 53, 4519–4525

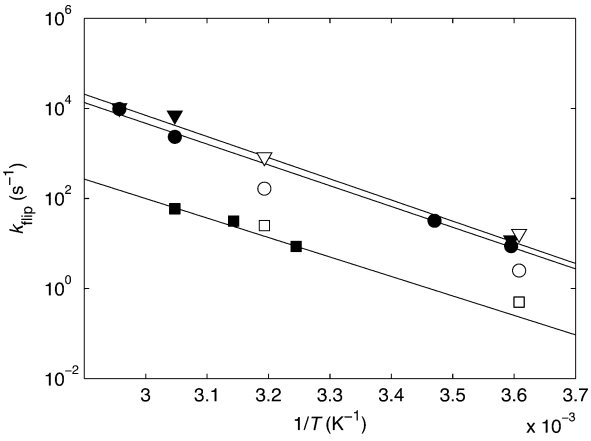

Figure 2. Temperature dependence of flip rates. k_{flip} plotted as a function of $1/T$ for Y23 (●), Y35 (■), and F45 (▼). For reference, data from previous studies[1] are shown as empty symbols. The data are represented using a logarithmic y-axis to show the expected linearity, but the fit was performed using nonlinear regression of k_{flip} on T.

heavily overlapped with Y23δ, which precludes quantitative analysis; however, the spectra clearly show that F22δ becomes broadened beyond detection at 5 °C (Figure S3 of the Supporting Information). Second, we find that the ring-flip model, with equal populations of exchanging sites, fits the data adequately. Parameter estimation using grid search shows that models with skewed populations ($p_1 \leq 0.1$) yield χ^2 values significantly higher than those of models for which $0.1 < p_1 \leq 0.5$. Exchange involving a highly populated alternative orientation of the F22 aromatic ring would be expected to affect other residues located nearby, but there is no evidence of conformational exchange in this region of the protein.[37,38] Third, the relatively slow flip rate of F22 is in agreement with a recent MD simulation,[26] as discussed further below, which further bolsters our interpretation of the relaxation dispersion in terms of ring flips.

BPTI is known to form decamers and higher-order oligomers at high protein and salt concentrations.[39] On the basis of data reported in the literature,[39] we estimate that the fraction of oligomers should be <5% under the sample conditions presented here. Thus, the small amount of oligomers possibly present is not expected to influence the ring-flip rates to any significant extent.

The Updated Rank Order of Ring-Flip Rates in BPTI Shows Qualitative Agreement with MD Results. Prior to our work, the most recent rank order of ring-flip rates in BPTI suggested that the rates could be listed from slow to fast as follows: Y35 ≪ Y23 < F45 ≪ F4 and F33 < Y10, Y21, and F22 [the latter five were estimated to flip quite fast ($k_{flip} > 10^6$ s^{-1})].[40] Our current results lead to a revised rank order of ring-flip rates: Y35 < Y21, Y23, and F45 < F22 < F4, Y10, and F33 (cf. Table 1). We stress that the rates for the last three residues in this list have not actually been measured but are inferred to be fast on the basis of the observation that the two nuclei on either side of the ring give rise to a single resonance line. The updated rank order is in much better agreement with the recent 1 ms MD trajectory[26] of BPTI than that based on previously reported data. Specifically, the MD-derived ranking in order of increasing rates is as follows: F45 (no observed ring flips) < Y21 and Y23 (1×10^3 s^{-1}) < Y35 (1×10^4 s^{-1}) < F22 (7×10^4 s^{-1}) < Y10 (1×10^6 s^{-1}), F33 (6×10^6 s^{-1}), and F4 (7×10^6 s^{-1}).[26] Similarly, in a 1.27 μs MD simulation at 375 K, the only rings that flipped were F4 (287 flips), Y10 (276 flips), F22 (6 flips), and F33 (34 flips).[40] All residues found by ^{13}C relaxation dispersion experiments to flip relatively slowly ($k_{flip} \leq 10^3$ s^{-1}) belong to the group of more slowly flipping rings ($k_{flip} \sim 10^3$–10^4 s^{-1}) in the 1 ms MD trajectory, while the three residues for which experimental rate measurements have not been achieved correspond to those that flip with rates of $\geq 10^6$ s^{-1} in the MD simulation. Thus, the new experimental data validate the MD trajectory in qualitative terms.

We note that the absolute rates derived from the MD trajectory show significant deviations from the experimental data. Except for the obvious anomaly of F45, which does not flip at all in the MD simulation, the rates for all slowly flipping residues are overestimated by 1–2 orders of magnitude. Specifically, Y35 shows a flip rate in the simulations considerably higher than that measured by experiment, 1×10^4 s^{-1} (at 27 °C) compared to 9 s^{-1} (at 35 °C). This discrepancy can be explained by the combination of two factors. First, the 1 ms MD trajectory of BPTI has revealed that the likelihood that a given aromatic ring undergoes a rotation around χ_2 depends strongly on the global state of the protein. Indeed, the flip rate of Y35 varies between 0 and 1.6×10^4 s^{-1} among the three most populated basins of the energy landscape, as a consequence of the variation between these basins in the local structure around Y35. By contrast, those rings that flip slowly in the MD simulation [Y21, Y23, and F45 ($k_{flip} \leq 10^3$ s^{-1})] are all located in a region of the protein that differs less in structure between alternative basins.[26] Second, the conformational sampling of basins along the MD trajectory does not reproduce the true equilibrium, as assessed by NMR;[27,28] this deviation is expected because the free energy differences between basins are within the limits of uncertainty of current force fields.[26] Givent that the MD-derived populations do not accurately represent the true equilibrium, it is not surprising that the effective flip rate of Y35 is overestimated by the MD simulation. Taken together, these results indicate encouraging agreement between experiment and simulation but also suggest that continued refinement of force fields and simulation methods is required to quantitatively reproduce the complex dynamics underlying aromatic ring rotations.

Measuring Faster Ring-Flip Rates Using ^{13}C $R_{1\rho}$ Relaxation Dispersion Experiments. To characterize the ring-flip dynamics at higher temperatures, where the exchange is too fast to be measured accurately by CPMG-type dispersion experiments, we used the ^{13}C L-TROSY $R_{1\rho}$ relaxation dispersion experiment.[23] At 55 °C, both Y23ε and F45δ have merged into single peaks. In both cases, CPMG methods are able to detect fast exchange but cannot be used to reliably quantify the rate. We acquired on-resonance ^{13}C $R_{1\rho}$ relaxation dispersion profiles at 55 and 65 °C, which reveal exchange for both Y23ε and F45δ (Figure 3). The free energy of unfolding (ΔG_U) of BPTI at 65 °C is 30 kJ/mol, as calculated from the Gibbs–Helmholtz equation and the reported thermal unfolding parameters (ΔH_U = 312 kJ/mol, ΔC_p = 1.3 kJ mol^{-1} K^{-1}, and T_m = 104 °C).[43] Hence, the population of unfolded species is insignificant over the entire temperature range covered here. To verify this expectation, we acquired ^{1}H–^{13}C HSQC spectra at temperatures of ≤75 °C, which did not reveal any peaks other than those from the folded protein (data not shown).

Similar to the CPMG relaxation dispersions, identical exchange rates were extracted regardless of whether the chemical shift differences were included as free parameters in

dx.doi.org/10.1021/bi500462k | Biochemistry 2014, 53, 4519–4525

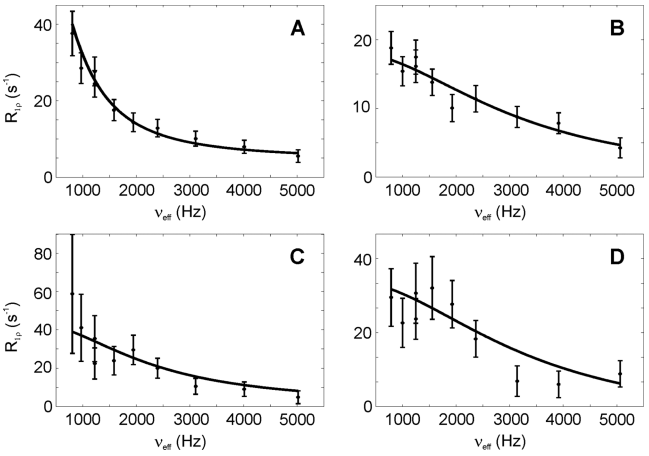

Figure 3. Aromatic ^{13}C L-TROSY-selected $R_{1\rho}$ relaxation dispersions of Y23ε (A and B) and F45δ (C and D) recorded on-resonance (tilt angle $\theta > 85°$) at a static magnetic field strength of 11.7 T at 55 °C (A and C) and 65 °C (B and D). Data were fit with fixed populations ($p_1 = p_2 = 0.5$) and free chemical shift differences ($\Delta\delta_{disp}$) and with the constraint k_{ex} (65 °C) > k_{ex} (55 °C). The resulting exchange rates (k_{ex}) are (A) (4.7 ± 0.9) × 10^3, (B) (19 ± 2) × 10^3, (C) (14 ± 4) × 10^3, and (D) (20 ± 3) × 10^3 s^{-1}.

the fit or fixed at the $\Delta\delta_{spectra}$ values (Figure S5 of the Supporting Information). The chemical shift differences determined from the fit show excellent agreement with those observed in spectra (Figure S4 of the Supporting Information), which further validates the ^{13}C L-TROSY $R_{1\rho}$ experiment.

Determining Activation Barriers from the Temperature Dependence of Flip Rates. To determine kinetic activation parameters of the ring flips, we analyzed flip rates as a function of temperature, covering the range from 5 to 65 °C.[43]The low effective concentration of ^{13}C sites at natural abundance, corresponding to 80 μM under the conditions presented here, imposes severe limitations on the achievable signal-to-noise ratio, which in turn restricts the range of temperatures at which high-quality relaxation dispersion profiles can be measured. For this reason, we were not able to perform measurements close to coalescence, where exchange broadening significantly reduces the signal intensities. Using a combination of CPMG and $R_{1\rho}$ experiments, data of sufficient quality were acquired across a range of temperatures for Y23, Y35, and F45, as follows: 5, 15, 55, and 65 °C for Y23; 35, 45, and 55 °C for Y35; and 5, 55, and 65 °C for F45 (see Table 1 and Figures S1, S2, and S5 of the Supporting Information). These data could be analyzed successfully to extract dynamic ring-flip parameters and subsequently used to determine activation parameters, as described below.

Figure 2 shows k_{flip} plotted logarithmically as a function of $1/T$ for Y23, Y35, and F45. As expected from theory, the plots are linear within experimental error. The results of the fits to the Eyring and Arrhenius equations are listed in Table 2. All three aromatic rings yield similar slopes in the plots of $\log(k_{flip})$ versus $1/T$; i.e., they have nearly identical energy barriers, $\Delta H^{\ddagger}$ or E_a. By contrast, the intercept is different for Y35 versus Y23 and F45, corresponding to a significantly lower value of $\Delta S^{\ddagger}$ (Table 2). Note that the chosen parametrization of the pre-exponential factor affects the fitted $\Delta S^{\ddagger}$. Here, we have used the gas-phase value, $k_B T/h$, thus assuming that the transmission coefficient is equal to 1 and hence identical among the different residues, which might not be the case in reality;[44] alternative

Table 2. Activation Parameters of Aromatic Ring Flips in BPTI

residue	E_a (kJ mol^{-1})[a]	$\Delta H^{\ddagger}$ (kJ mol^{-1})[b]	$\Delta S^{\ddagger}$ (J K^{-1} mol^{-1})[b]
Y23	88 ± 1	86 ± 3	81 ± 9
Y35	82.8 ± 0.5	83 ± 3	41 ± 10
F45	90 ± 2	86 ± 3	86 ± 10

[a]Obtained by nonlinear least-squares fits of k_{flip} vs T using the Arrhenius equation. [b]Obtained by nonlinear least-squares fits of k_{flip} vs T using the Eyring equation.

interpretations of the variations in the intercept are thus possible.

The activation parameters obtained for Y23 and F45 are identical within error, suggesting that the structural fluctuations governing the ring flips of these two residues are similar in character. This result is rationalized by the fact that Y23 and F45 are located in the same structural region (Figure 4). Y35

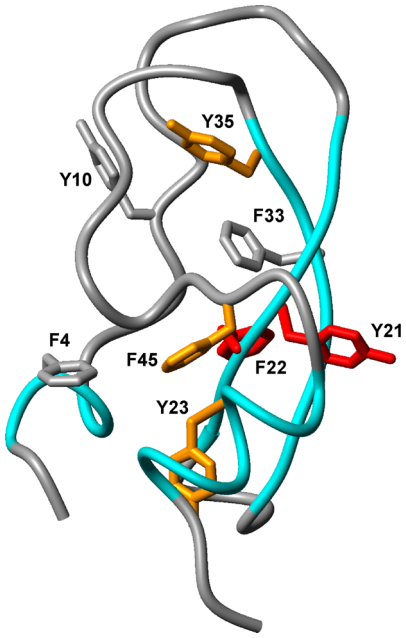

Figure 4. Three-dimensional structure of BPTI (Protein Data Bank entry 5pti[41]) showing the backbone and aromatic side chains as tubes and sticks, respectively. Secondary structure elements are colored cyan. Aromatic side chains are labeled by residue number. Slowly flipping rings ($k_{flip} < 10^3$ s^{-1}) identified by NMR are colored red [newly identified ones, F22 (this work) and Y21[15]] and orange (previously identified ones[1]). Rings not identified by experiment to flip slowly are colored gray. This figure was prepared using MOLMOL.[42]

differs from Y23 and F45 in $\Delta S^{\ddagger}$ and is located in a different region of the structure, which was shown to vary significantly between alternative basins sampled in the 1 ms MD simulation,[26] as described above. It is conceivable that the sampling of multiple ground-state conformations in this region of BPTI affects the $\Delta S^{\ddagger}$ of the Y35 ring flip.

The extracted values of $\Delta H^{\ddagger}$ range between 83 and 86 kJ mol^{-1}. These values fall within the limits of previously published results for other proteins, which range between 64 and 151 kJ mol^{-1}. The lower end of this range is represented by Y97 in cytochrome *c*, which exhibits significant curvature in the Arrhenius plot.[9] The highest value was obtained for Y67 in iso-2-cytochrome *c*, while Y46 and Y48 in the same protein both

dx.doi.org/10.1021/bi500462k | *Biochemistry* 2014, 53, 4519−4525

have $\Delta H^{\ddagger}$ values of 117 kJ mol^{-1}.[10] The high activation barriers observed for iso-2-cytochrome *c* might be explained by the structure: the rings of Y46 and Y48 pack tightly together in a typical aromatic-pair interaction, while Y67 packs against the heme group. Presumably, significant rearrangements of an extended region of the protein core are required for ring flips to take place in these cases. Our results for BPTI are highly comparable to recent data for Y6 in HPr, which yielded a $\Delta H^{\ddagger}$ of 89 ± 10 kJ mol^{-1}.[12]

We note that the relatively uniform activation barriers determined herein are in contrast with previous experimental results for BPTI, for which a greater range of activation enthalpies were obtained, varying from 59 to 155 kJ mol^{-1}.[1,6] The highest value was obtained for Y35, while Y23 yielded a $\Delta H^{\ddagger}$ of 109 kJ mol^{-1}, which is more in line with our current results. The lowest value, observed for F45, was recently determined by ^{1}H−^{1}H EXSY experiments conducted between −16.5 and −3.5 °C.[6] The observed differences between these results and previous results for F45 could conceivably be due to the difference in temperature, although the low-temperature results actually agree well with earlier data from ^{1}H line shape analysis covering the temperature range of 4−72 °C.[1] These discrepancies merit future investigation, which preferably should be conducted using isotope-enriched samples to ensure improved sensitivity and enhanced sampling of the temperature dependence.

■ ASSOCIATED CONTENT

Supporting Information

Table listing fitted exchange rates and chemical shift differences, figures showing all relaxation dispersion profiles, aromatic regions of the ^{1}H−^{13}C HSQC spectrum of BPTI, and a correlation plot comparing chemical shift differences between exchanging sites, as determined from the relaxation dispersion profiles or measured in the HSQC. This material is available free of charge via the Internet at http://pubs.acs.org.

■ AUTHOR INFORMATION

Corresponding Author

*E-mail: mikael.akke@bpc.lu.se.

Funding

This research was supported by the Swedish Research Council (621-2010-4912 and 822-2005-2915), the Göran Gustafsson Foundation for Research in Natural Sciences and Medicine, and the Knut and Alice Wallenberg Foundation. U.W. was supported by an EMBO long-term fellowship.

Notes

The authors declare no competing financial interest.

■ ACKNOWLEDGMENTS

We thank Bertil Halle for the BPTI sample.

■ ABBREVIATIONS

BPTI, basic pancreatic trypsin inhibitor; CPMG, Carr−Purcell−Meiboom−Gill; HPr, histidine-containing phosphocarrier protein; $R_{1\rho}$, rotating-frame relaxation.

■ REFERENCES

(1) Wagner, G., Demarco, A., and Wüthrich, K. (1976) Dynamics of Aromatic Amino-Acid Residues in Globular Conformation of Basic Pancreatic Trypsin-Inhibitor (BPTI). 1. H-1 NMR Studies. *Biophys. Struct. Mech. 2*, 139−158.

(2) Wagner, G., and Wüthrich, K. (1978) Dynamic Model of Globular Protein Conformations Based on NMR Studies in Solution. *Nature 275*, 247−248.

(3) Wagner, G. (1980) Activation Volumes ΔV Not Equal for the Rotational Flips of Internal Aromatic Rings in Globular-Proteins, Determined by High-Resolution 360-MHz H-1 NMR at Variable Pressure. *Experientia 36*, 735−735.

(4) Wagner, G., Brühwiler, D., and Wüthrich, K. (1987) Reinvestigation of the Aromatic Side-Chains in the Basic Pancreatic Trypsin-Inhibitor by Heteronuclear Two-Dimensional Nuclear-Magnetic-Resonance. *J. Mol. Biol. 196*, 227−231.

(5) Li, H., Yamada, H., and Akasaka, K. (1999) Effect of pressure on the tertiary structure and dynamics of folded basic pancreatic trypsin inhibitor. *Biophys. J. 77*, 2801−2812.

(6) Skalicky, J. J., Mills, J. L., Sharma, S., and Szyperski, T. (2001) Aromatic ring-flipping in supercooled water: Implications for NMR-based structural biology of proteins. *J. Am. Chem. Soc. 123*, 388−397.

(7) Dobson, C. M., Moore, G. R., and Williams, R. J. P. (1975) Assignment of Aromatic Amino-Acid PMR Resonances of Horse Ferricytochrome c. *FEBS Lett. 51*, 60−65.

(8) Campbell, I. D., Dobson, C. M., Moore, G. R., Perkins, S. J., and Williams, R. J. P. (1976) Temperature-Dependent Molecular-Motion of a Tyrosine Residue of Ferrocytochrome c. *FEBS Lett. 70*, 96−100.

(9) Rao, D. K., and Bhuyan, A. K. (2007) Complexity of aromatic ring-flip motions in proteins: Y97 ring dynamics in cytochrome c observed by cross-relaxation suppressed exchange NMR spectroscopy. *J. Biomol. NMR 39*, 187−196.

(10) Nall, B. T., and Zuniga, E. H. (1990) Rates and Energetics of Tyrosine Ring Flips in Yeast Iso-2-Cytochrome c. *Biochemistry 29*, 7576−7584.

(11) Campbell, I. D., Dobson, C. M., and Williams, R. J. P. (1975) Proton magnetic resonance studies of the tyrosine residues of hen lysozyme: Assignment and detection of conformational mobility. *Proc. R. Soc. B 189*, 503−509.

(12) Hattori, M., Li, H., Yamada, H., Akasaka, K., Hengstenberg, W., Gronwald, W., and Kalbitzer, H. R. (2004) Infrequent cavity-forming fluctuations in HPr from *Staphylococcus carnosus* revealed by pressure- and temperature-dependent tyrosine ring flips. *Protein Sci. 13*, 3104−3114.

(13) Baturin, S. J., Okon, M., and McIntosh, L. P. (2011) Structure, dynamics, and ionization equilibria of the tyrosine residues in *Bacillus circulans* xylanase. *J. Biomol. NMR 51*, 379−394.

(14) Ulrich, E. L., Akutsu, H., Doreleijers, J. F., Harano, Y., Ioannidis, Y. E., Lin, J., Livny, M., Mading, S., Maziuk, D., Miller, Z., Nakatani, E., Schulte, C. F., Tolmie, D. E., Wenger, R. K., Yao, H. Y., and Markley, J. L. (2008) BioMagResBank. *Nucleic Acids Res. 36*, D402−D408.

(15) Weininger, U., Respondek, M., Löw, C., and Akke, M. (2013) Slow Aromatic Ring Flips Detected Despite Near-Degenerate NMR Frequencies of the Exchanging Nuclei. *J. Phys. Chem. B 117*, 9241−9247.

(16) Akke, M. (2002) NMR methods for characterizing microsecond-millisecond dynamics in recognition and catalysis. *Curr. Opin. Struct. Biol. 12*, 642−647.

(17) Palmer, A. G., and Massi, F. (2006) Characterization of the dynamics of biomacromolecules using rotating-frame spin relaxation NMR spectroscopy. *Chem. Rev. 106*, 1700−1719.

(18) Palmer, A. G., Kroenke, C. D., and Loria, J. P. (2001) Nuclear magnetic resonance methods for quantifying microsecond-to-millisecond motions in biological macromolecules. *Methods Enzymol. 339*, 204−238.

(19) Teilum, K., Brath, U., Lundström, P., and Akke, M. (2006) Biosynthetic ^{13}C labeling of aromatic side-chains in proteins for NMR relaxation measurements. *J. Am. Chem. Soc. 128*, 2506−2507.

(20) Lundström, P., Teilum, K., Carstensen, T., Bezsonova, I., Wiesner, S., Hansen, F., Religa, T. L., Akke, M., and Kay, L. E. (2007) Fractional ^{13}C enrichment of isolated carbons using [1-^{13}C]- or [2-^{13}C]-glucose facilitates the accurate measurement of dynamics at backbone Ca and side-chain methyl positions in proteins. *J. Biomol. NMR 38*, 199−122.

(21) Kasinath, V., Valentine, K. G., and Wand, A. J. (2013) A ^{13}C labeling strategy reveals a range of aromatic side chain motion in calmodulin. *J. Am. Chem. Soc. 135*, 9560−9563.
(22) Weininger, U., Respondek, M., and Akke, M. (2012) Conformational exchange of aromatic side chains characterized by L-optimized TROSY-selected ^{13}C CPMG relaxation dispersion. *J. Biomol. NMR 54*, 9−14.
(23) Weininger, U., Brath, U., Modig, K., Teilum, K., and Akke, M. (2014) Off-resonance rotating-frame relaxation dispersion experiment for ^{13}C in aromatic side chains using L-optimized TROSY-selection. *J. Biomol. NMR 59*, 23−29.
(24) Hetzel, R., Wuthrich, K., Deisenhofer, J., and Huber, R. (1976) Dynamics of Aromatic Amino-Acid Residues in Globular Conformation of Basic Pancreatic Trypsin-Inhibitor (BPTI). 2. Semiempirical Energy Calculations. *Biophys. Struct. Mech. 2*, 159−180.
(25) Gelin, B. R., and Karplus, M. (1975) Sidechain Torsional Potentials and Motion of Amino-Acids in Proteins: Bovine Pancreatic Trypsin-Inhibitor. *Proc. Natl. Acad. Sci. U.S.A. 72*, 2002−2006.
(26) Shaw, D. E., Maragakis, P., Lindorff-Larsen, K., Piana, S., Dror, R. O., Eastwood, M. P., Bank, J. A., Jumper, J. M., Salmon, J. K., Shan, Y. B., and Wriggers, W. (2010) Atomic-Level Characterization of the Structural Dynamics of Proteins. *Science 330*, 341−346.
(27) Persson, F., and Halle, B. (2013) Transient Access to the Protein Interior: Simulation versus NMR. *J. Am. Chem. Soc. 135*, 8735−8748.
(28) Xue, Y., Ward, J. M., Yuwen, T. R., Podkorytov, I. S., and Skrynnikov, N. R. (2012) Microsecond Time-Scale Conformational Exchange in Proteins: Using Long Molecular Dynamics Trajectory To Simulate NMR Relaxation Dispersion Data. *J. Am. Chem. Soc. 134*, 2555−2562.
(29) Delaglio, F., Grzesiek, S., Vuister, G. W., Zhu, G., Pfeifer, J., and Bax, A. (1995) NMRPipe: A multidimensional spectral processing system based on UNIX pipes. *J. Biomol. NMR 6*, 277−293.
(30) Johnson, B. A. (2004) Using NMRView to visualize and analyze the NMR spectra of macromolecules. *Methods Mol. Biol. 278*, 313−352.
(31) Carver, J. P., and Richards, R. E. (1972) A general two-site solution for the chemical exchange produced dependence of T_2 upon the Carr-Purcell pulse separation. *J. Magn. Reson. 6*, 89−105.
(32) Davis, D. G., Perlman, M. E., and London, R. E. (1994) Direct measurements of the dissociation-rate constant for inhibitor-enzyme complexes via the T_{1r} and T_2 (CPMG) methods. *J. Magn. Reson., Ser. B 104*, 266−275.
(33) Gutowsky, H. S., Vold, R. L., and Wells, E. J. (1965) Theory of chemical exchange effects in magnetic resonance. *J. Chem. Phys. 43*, 4107−4125.
(34) Tollinger, M., Skrynnikov, N. R., Mulder, F. A. A., Forman-Kay, J. D., and Kay, L. E. (2001) Slow dynamics in folded and unfolded states of an SH3 domain. *J. Am. Chem. Soc. 123*, 11341−11352.
(35) Press, W. H., Flannery, B. P., Teukolsky, S. A., and Vetterling, W. T. (1986) Numerical Recipes. *The Art of Scientific Computing*, Cambridge University Press, Cambridge, U.K.
(36) Miloushev, V. Z., and Palmer, A. G. (2005) $R_{1\rho}$ relaxation for two-site chemical exchange: General approximations and some exact solutions. *J. Magn. Reson. 177*, 221−227.
(37) Szyperski, T., Luginbühl, P., Otting, G., Güntert, P., and Wüthrich, K. (1993) Protein dynamics studied by rotating frame ^{15}N spin relaxation times. *J. Biomol. NMR 3*, 151−164.
(38) Grey, M. J., Wang, C., and Palmer, A. G. (2003) Disulfide bond isomerization in basic pancreatic trypsin inhibitor: Multisite chemical exchange quantified by CPMG relaxation dispersion and chemical shift modeling. *J. Am. Chem. Soc. 125*, 14324−14335.
(39) Gottschalk, M., Venu, K., and Halle, B. (2003) Protein self-association in solution: The bovine pancreatic trypsin inhibitor decamer. *Biophys. J. 84*, 3941−3958.
(40) Sathyamoorthy, B., Singarapu, K. K., Garcia, A. E., and Szyperski, T. (2013) Protein conformational space populated in solution probed with aromatic residual dipolar ^{13}C-^{1}H couplings. *ChemBioChem 14*, 685−688.
(41) Wlodawer, A., Walter, J., Huber, R., and Sjolin, L. (1984) Structure of bovine pancreatic trypsin inhibitor. Results of joint neutron and X-ray refinement of crystal form II. *J. Mol. Biol. 180*, 301−329.
(42) Koradi, R., Billeter, M., and Wüthrich, K. (1996) MOLMOL: A program for display and analysis of macromolecular structures. *J. Mol. Graphics 14*, 51−55.
(43) Makhatadze, G. I., Kim, K. S., Woodward, C., and Privalov, P. L. (1993) Thermodynamics of BPTI Folding. *Protein Sci. 2*, 2028−2036.
(44) Karplus, M. (2000) Aspects of protein reaction dynamics: Deviations from simple behavior. *J. Phys. Chem. B 104*, 11−27.